Earth and Planetary Science Letters 534 (2020) 116083

Contents lists available at ScienceDirect

Earth and Planetary Science Letters

www.elsevier.com/locate/epsl

Molybdenum isotope fractionation in glacial diamictites tracks the onset of oxidative weathering of the continental crust

Allison T. Greaney [a,*,1], Roberta L. Rudnick [a,b], Stephen J. Romaniello [c,d], Aleisha C. Johnson [c], Richard M. Gaschnig [e], Ariel D. Anbar [c,f]

[a] Department of Earth Science and Earth Research Institute, University of California - Santa Barbara, Santa Barbara, CA 93106, United States of America
[b] Department of Geology, University of Maryland - College Park, College Park, MD 20742, United States of America
[c] School of Earth and Space Exploration, Arizona State University, Tempe, AZ 85281, United States of America
[d] Department of Earth and Planetary Sciences, University of Tennessee - Knoxville, Knoxville, TN 37996, United States of America
[e] Department of Environmental, Earth and Atmospheric Sciences, University of Massachusetts - Lowell, Lowell, MA 01854, United States of America
[f] School of Molecular Sciences, Arizona State University, Tempe, AZ 85281, United States of America

ARTICLE INFO

Article history:
Received 2 June 2019
Received in revised form 5 January 2020
Accepted 8 January 2020
Available online 27 January 2020
Editor: I. Halevy

Keywords:
molybdenum
great oxidation event
weathering
isotope fractionation
continental crust

ABSTRACT

Molybdenum isotopes in twenty-four composites of glacial diamictites spanning depositional ages of 2900 to 300 Ma show a systematic shift to lighter compositions and a decrease in Mo concentration over time. The diamictites fall into three age groups relative to the Great Oxidation Event (GOE): pre-GOE (2.43 – 2.90 Ga), syn-GOE (2.20 – 2.39 Ga), and post-GOE (0.33 – 0.75 Ga). Pre-GOE composites have an average $\delta^{98}Mo_{NIST3134}$ of +0.03‰ (± 0.18‰), syn-GOE composites average −0.29‰ (± 0.60‰), and post-GOE composites average −0.45‰ (± 0.51‰). These groups are statistically different at p=0.05. We use the pre-GOE data to estimate the average Archean upper continental crust (UCC) δ^{98}Mo signature as +0.03 ± 0.18‰ (2σ), which falls within the range of previous estimates of modern igneous rocks. As the diamictites represent a mixture of igneous and weathered crust, the shift to lighter Mo values over time likely reflects Mo isotope fractionation during oxidative weathering and increased retention of light Mo isotopes in weathered regolith and soils. We hypothesize that this fractionation is due to the mobilization of oxidized Mo following the GOE, and subsequent adsorption of light Mo onto Fe-Mn oxides and/or organic matter in weathered regolith. We conclude that Mo isotopes in continental weathering products record the rise of atmospheric oxygen and onset of oxidative weathering. As the regolith formed under oxidative conditions is isotopically lighter than average continental igneous rocks, mass balance dictates that Mo isotope fractionation during oxidative weathering should result in isotopically heavy groundwater and river water, which is observed in modern systems.

1. Introduction

Molybdenum concentrations and isotope compositions in sedimentary rocks are powerful proxies used to infer the oxidation state of the ancient atmosphere and oceans, due to the redox sensitivity of Mo (Anbar et al., 2007; Barling et al., 2001; Siebert et al., 2003). Within the unweathered UCC, up to 60% of Mo may reside in hydrothermal molybdenite (MoS_2) (Greaney et al., 2018). Therefore, a significant fraction of UCC Mo is hosted in a mineral that is susceptible to oxidative weathering following the Great Oxidation Event (GOE) (Anbar et al., 2007; Johnson et al., 2019). Alternatively, Mo may be hosted primarily in volcanic glass or Ti-bearing phases in the UCC (Greaney et al., 2018). A recent study of the residence of Mo in the glacial diamictites studied here indicates that molybdenite may not have been a significant host of Mo in the UCC prior to the GOE (Li et al., 2019). In any case, once liberated from its mineralogical or glassy host and oxidized, Mo is removed from the UCC via transport in groundwater to rivers and oceans.

Molybdenum is a unique redox proxy because it is not only sensitive to the presence of O_2, but also to the presence of Fe-Mn oxides and organic matter in the weathering environment. Sedimentary records of molybdenum isotopes can therefore elucidate the nature of the GOE, as well as its impact in reshaping the terrestrial biosphere preceding the evolution of eukaryotes and animals.

* Corresponding author.
E-mail address: greaneyat@ornl.gov (A.T. Greaney).
[1] Now at Oak Ridge National Laboratory, 1 Bethel Valley Road, Oak Ridge, TN 37830.

https://doi.org/10.1016/j.epsl.2020.116083
0012-821X/

1.1. Mo isotope fractionation during continental weathering

Dissolved Mo in modern rivers is isotopically heavy relative to the UCC, with a range of δ^{98}Mo between +0.2 and +2.3‰$_{NIST3134}$ (Archer and Vance, 2008). Some researchers suggest this offset from crustal values results from adsorption of light Mo isotopes onto oxides in soils and river sediments during continental weathering (Archer and Vance, 2008; Pearce et al., 2010). Others propose that there is no net fractionation during weathering, and that average riverine values reflect weathering of a source that's heavier than average continental crust, e.g., molybdenite (Dahl et al., 2011; Neubert et al., 2011). However, molybdenite shows a wide range of δ^{98}Mo values from -1.5 to 2.4‰, with an average of 0.04‰ ± 1.04 (2σ) (Breillat et al., 2014), which is similar to average igneous rocks (Kendall et al., 2017; Willbold and Elliott, 2017).

Recent studies have addressed Mo isotope fractionation during weathering on several types of bedrock to determine the magnitude of fractionation and the species responsible for inducing fractionation. Wang et al. (2018) analyzed a saprolite weathering profile formed on granite and found that Mo isotopes in the soil are generally lighter than the bedrock. The majority of light Mo in the soils is associated with Fe-(hyr)-oxides, as opposed to clays and organic matter, which were also present. This study concluded that Fe-Mn oxides in soils preferentially retain light Mo, thereby leaving the complementary ground- and river-water isotopically heavy. Molybdenum isotope fractionation during adsorption onto Fe-Mn oxides has been well established in natural settings (Barling et al., 2001; Siebert et al., 2003) and laboratory experiments (Barling and Anbar, 2004; Goldberg et al., 2009; Wasylenki et al., 2008).

Recent work has also shown that Mo isotopes can be fractionated by adsorption onto organic matter in the same direction and to the same degree as by adsorption onto Fe-Mn oxides. Organic matter (OM) retains lighter Mo isotopes with similar fractionation factors to those oxides, calculated as α = fluid/oxide: humic acid (organic matter), α = 1.0017, King et al., 2018; Fe-Mn oxides $1.0004 < \alpha < 1.0027$, Goldberg et al., 2009 and Wasylenki et al., 2008. In a study of basaltic weathering profiles from Hawaii, Iceland, and Costa Rica, Siebert et al. (2015) conclude that processes other than Mo adsorption onto Fe-Mn oxides (e.g., organic matter fractionation) may disrupt the expected fractionation due to adsorption onto oxides. Additionally, King et al. (2016) found that while Hawaiian soils are typically lighter than the parental bedrock, there is no correlation between δ^{98}Mo and oxide content of the soil. Therefore, these authors propose that atmospheric inputs and Mo complexation with organic matter may have a more significant fractionation effect than Mo adsorption onto oxides. A mass balance for Mo in forest soils shows that organic matter can retain 40 times more Mo than Fe-Mn oxides (Marks et al., 2015). Thus, organic matter may be an important host of isotopically light Mo in the regolith, in addition to Fe-Mn oxides.

1.2. Glacial diamictites record continental weathering

To assess whether Mo isotopes are fractionated during continental weathering and whether the nature of weathering varies throughout Earth's history, we turn to glacial diamictites. V.M. Goldschmidt first proposed the use of glacial deposits as a means of obtaining a geochemical average of the UCC. As glaciers move over the exposed crust, they erode the uppermost weathered regolith and un-weathered crust beneath it, generating sediments that effectively average out large surface areas of the continents. These sediments are then deposited as "diamictites" on shallow marine continental margins or in subaerial glacial tills. Assuming the diamictites are not greatly weathered or altered after deposition by the glacier, as discussed below, they record the chemical weathering signature of the UCC at the time of glaciation. These signatures provide a unique window on studying past interactions between the atmosphere and upper crust.

Gaschnig et al. (2014) presented data for 122 individual glacial diamictites from 27 formations that span the last 2.9 billion years of Earth's history and Gaschnig et al. (2016) created 24 composites of the complete sample set by combining multiple diamictite samples from the same formation. These studies found that the diamictites show a weathering signature regardless of the age of the sample. This weathering signature is recorded by Sr loss from nearly all samples as exhibited by low relative Sr concentrations (quantified as Sr/Sr* (Sr/Sr*=Sr/(Ce*Pr)$^{0.5}$) and an elevated chemical index of alteration (CIA). The weathering signature of the diamictites was determined to have been inherited from the source as there is little to no evidence of post-depositional weathering or alteration, e.g., formation of paleosols or weathering profiles on top of the deposits (Gaschnig et al., 2014). Additionally, Li isotopes, which are strongly fractionated during continental weathering, do not show systematic changes downward in the diamictite units (Li et al., 2016). However, the diamictites have undergone low grade metamorphism, so the current mineralogy may not be reflective of original deposition. Thus, diamictites provide a geochemical average of the weathered UCC and can be used to understand chemical weathering of Archean and Proterozoic crust.

The diamictites also record the rise of atmospheric oxygen. Gaschnig et al., 2014 also found that Mo and other Redox Sensitive Elements (e.g., V) are notably depleted relative to insoluble elements in the diamictites that formed after the GOE, suggesting that Mo was removed due to oxidative weathering. If the conclusions of these prior studies are correct and the behavior of Mo in the weathered crust is affected by atmospheric chemistry, then isotope fractionation is likely to occur as well.

In this study, we use these diamictite composites to provide new, independent constraints on Mo fractionation during continental weathering and find that Mo isotopes in the weathered crust to record changes in atmospheric chemistry and/or soil redox over much of Earth's history. These composites have been analyzed for major and trace elements and oxygen isotopes (Gaschnig et al., 2016), Li isotopes to assess the presence of secondary alteration (Li et al., 2016), and several other stable isotopes. The composites are analyzed here for Mo isotopes and total organic carbon (TOC) to determine the effect of Mo complexation with organic matter on overall Mo isotope fractionation during weathering. The samples span four modern continents and range in age from 2900 to 300 Ma, and record the weathering signature at the time of glaciation (Gaschnig et al., 2014, 2016).

2. Methods

Twenty four diamictite composites were created by Gaschnig et al. (2016) from the complete sample set analyzed in Gaschnig et al. (2014). These composites were made by separating the fine-grained diamictite matrix from each individual sample, powdering it, and mixing with powdered matrix material from other diamictite samples from the same formation. To prevent contamination of trace metals, initial removal of the diamictite clasts from the matrix was accomplished by hammering the rock between thick plastic sheets and separating matrix from clasts by hand; powdering of the matrix was undertaken using a ceramic jaw crusher and disk mill (Gaschnig et al., 2014).

Molybdenum isotope data were collected at the W.M. Keck Laboratory for Environmental Biogeochemistry at Arizona State University using the double spike method presented in Romaniello et al. (2016). Sample aliquots containing 75 ng of Mo (between 30 and 300 mg of sample powder) were ashed at 550°C in a furnace overnight to remove organics. Powders were transferred to Savillex beakers and dissolved on a hotplate using a mixture of 5 mL of

Table 1
Mo isotope and select major and trace element data for the diamictite composites. All major and trace element data can be found in Gaschnig et al. (2016). See supplementary table S1 for references on the age and geologic setting on the diamictites.

Sample	Country	Age (Ma*)	Relative GOE	δ^{98}Mo (‰)	2SD	TOC (wt%)	Mo† (ppm)
Mozaan Group	S. Africa	2965	pre	0.04	0.04	0.06	0.884
Afrikander Frm	S. Africa	2960	pre	0.16	0.10	0.03	0.471
Coronation Frm	S. Africa	2960	pre	-0.02	0.04	0.08	2.97
Promise Frm	S. Africa	2960	pre	-0.05	0.04	0.08	0.774
Ramsay Lake Frm	Canada (Ontario)	2436	pre	-0.07	0.04	0.07	2.29
Makganyene Frm	S. Africa	2436	pre	0.10	0.04	0.15	1.04
Bruce Frm	Canada (Ontario)	2380	syn	-0.21	0.04	0.05	1.46
Duitschland Frm	S. Africa	2380	syn	-0.80	0.06	0.12	0.547
Gowganda Frm	Canada (Ontario)	2350	syn	-0.15	0.05	0.06	1.78
Bottle Creek Frm	USA (Wyoming)	2275	syn	-0.28	0.05	0.05	0.578
Timeball Hill Frm	S. Africa	2250	syn	-0.01	0.04	0.15	1.3
Kaigas Frm	Namibia	755	post	-0.20	0.04	0.08	1.01
Konnarock Frm	USA (Virginia)	665	post	-0.65	0.04	0.05	0.478
Gaskiers Frm	Canada (Newfoundland)	580	post	-0.57	0.04	0.06	0.559
Pocatello Frm	USA (Idaho)	685	post	-0.45	0.04	0.07	1.17
Nantuo Frm	China (Hubei)	645	post	-0.75	0.11	0.09	0.317
Gucheng Frm	China (Hubei)	680	post	-0.72	0.07	0.19	0.332
Blaubeker Frm	Namibia	693	post	-0.36	0.04	0.05	0.49
Chuos Frm	Namibia	690	post	-0.52	0.04	0.11	0.614
Numees Frm	Namibia	650	post	-0.27	0.04	0.10	0.425
Ghaub Frm	Namibia	635	post	-0.05	0.06	0.11	0.463
Bolivia Group	Bolivia	315	post	-0.19	0.04	0.26	0.239
Dwyka East	S. Africa & Namibia	300	post	-0.27	0.04	0.15	0.73
Dwyka West	S. Africa & Namibia	300	post	-0.89	0.04	0.31	2.88

* Ages are averages of min and max dates provided by references, therefore should not be considered exact. Syn-GOE ages are estimated based on published ages and stratigraphic constraints relative to oxidatve weathering signature (see Gumsley et al., 2017).

† From Gaschnig et al. (2016).

concentrated HNO_3 and between 1 and 2 mL of concentrated HF, depending on the silica content of the samples. Immediately prior to dissolution, a ^{97}Mo-^{100}Mo double spike was added to the powders to produce a constant 2:1 ratio between the double-spike and sample-derived Mo (Mo concentrations taken from Gaschnig et al., 2016). After two days of hot plate dissolution, the solutions were evaporated to near-dryness and re-fluxed twice overnight in 1 mL of concentrated HCl to produce a clear solution free of precipitates. Finally, the samples were dried down and brought up in 1 mL of 6M HCl for column chemistry.

Mo was purified from the sample matrix using a combination of anion and cation exchange chromatography. For the anion column method, 2 mL of cleaned Biorad AG1X-8 anion exchange resin were loaded into the columns and rinsed with 10 mL of 1 M HCl. Twenty mL of 6 M HCl was run through the columns for equilibration, the samples (in 6M HCl) were loaded, and the sample was rinsed repeatedly with 6M HCl. Sample elution was achieved using repeated aliquots of increasing volumes of 1 M HCl, from 0.5 mL up to 10 mL. The eluent was dried down and brought up in 6 M HCl and the anion column chemistry was repeated a second time. After the second round, samples were brought up in 0.5 M HCl. Biorad AG50WX-8 cation exchange resin was used for cation column chemistry. Two mLs of resin were loaded into the column then cleaned and equilibrated overnight in 10 mL of 0.5 M HCl. Afterwards, 10 mL of 0.5 M HCl + 0.01% H_2O_2 were added to the columns in order to keep Mo oxidized. The samples were loaded into the columns and Mo was eluted with repeated volumes of 0.5 M HCl + 0.01% H_2O_2 from 0.5 mL up to 10 mL. The final eluate was dried down and samples were refluxed in 1 mL of concentrated HNO_3 + 200 µL of H_2O_2 twice to oxidize any remaining organic residue. Finally, the samples were dried down and brought up in 3 mL of 2% HNO_3 for analysis. These methods were developed by Barling et al. (2001), Duan et al. (2010), G. Gordon in Goldberg et al. (2013), Romaniello et al. (2016) and additional references therein.

The isotopes ^{91}Zr, ^{92}Mo, ^{95}Mo, ^{96}Mo, ^{97}Mo, ^{98}Mo, ^{99}Ru, and ^{100}Mo were measured on the Thermo-Neptune Multi-collector ICP-MS on three sample aliquots of ~25 ng Mo. Mass-99 was monitored to check for high organic content that could interfere with Mo measurements (Goldberg et al., 2013). A double spike inversion was performed using an in-house MATLAB script at ASU which uses non-linear least squares optimization to simultaneously solve for the spike-sample ratio, instrument mass bias, and isotopic fractionation of the samples. Mo isotope data are reported as: $\delta^{98}Mo = 1000*[(^{98}Mo/^{95}Mo_{sample})/(^{98}Mo/^{95}Mo_{standard})-1]$ relative to the isotopic composition of NIST 3134 Mo standard (**Table 1**). The USGS shale SDO-1 was analyzed as a secondary standard and yielded a value of 0.79‰ (±0.03 2σ), in excellent agreement with published values (Goldberg et al., 2013). Additionally, the USGS rhyolite RGM-1 was run as a secondary standard and produced a value of +0.3‰ (±0.01 2σ). Internal run precision and long-term precision are both around 0.04‰.

Organic C measurements were made at the University of Maryland. The samples were repeatedly washed in 3M HCl and then Millipore 18Ω water to remove carbonate C and bring the sample to near neutral pH, respectively. The samples were then dried in an oven at 80°C for two days. Aliquots of between 5 and 15 mg of sample were loaded in tin cups, then combusted and analyzed using an Eurovector element analyzer. Carbon abundances of the aliquots were determined against a urea standard and TOC abundance (wt%) for whole rock sample was calculated using the proportion of carbonate removed during acid washing.

3. Results

The diamictite samples are divided into three groups based on their stratigraphic ages: diamictites deposited before the GOE ("pre-GOE", 2430 – 2900 Ma), those deposited during or just after the GOE ("syn-GOE", 2200 – 2380 Ma), and those deposited significantly after the GOE in the Neoproterozoic/Phanerozoic (la-

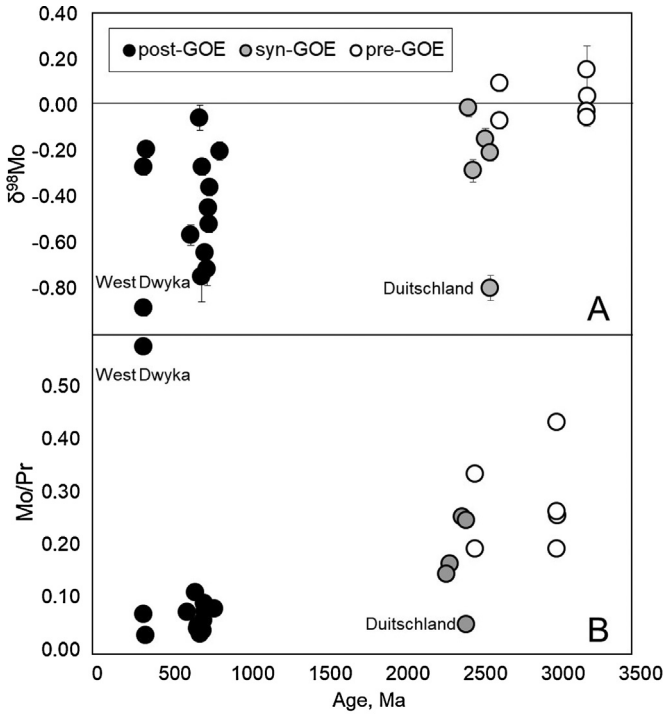

Fig. 1. δ^{98}Mo and Mo/Pr of the glacial diamictites plotted as a function of depositional age. Error bars on 1A represent in-run precision (2σ), which is similar to the long-term precision. Error bars on 1B are within the data point.

belled "post-GOE", 300 – 755 Ma) (age references can be found in the supplementary table; many stratigraphic constraints are taken from Gumsley et al., 2017). The pre-GOE samples have an average δ^{98}Mo signature of +0.03 ± 0.18 ‰ (2σ). The syn-GOE samples (average −0.29 ± 0.60‰) and the post-GOE samples (average −0.45 ± 0.51‰) are isotopically lighter than the pre-GOE samples (**Fig. 1A**). The Mo/Pr ratio can be used to track the behavior of Mo during weathering relative to Pr, as the two elements generally behave similarly during igneous processes (Gaschnig et al., 2014). Therefore, a change in Mo/Pr of the diamictite composites suggests that Mo is decoupled from Pr during weathering. As the δ^{98}Mo of the diamictites decreases over time, the Mo/Pr ratio decreases from an average of 0.28 ± 0.18 2σ (pre-GOE) to 0.17 ± 0.19 (syn-GOE) and finally to an average of 0.10 ± 0.29 in the post-GOE samples (**Fig. 1B**). The large post-GOE error reflects the outlier sample, West Dwyka. The decreasing Mo/Pr ratio results from a decreasing average [Mo] over time (pre-GOE = 1.4 ppm, syn-GOE = 1.1 ppm, post-GOE = 0.75 ppm) as well as an increase in Pr over time. While these absolute concentrations may be diluted by the presence of quartz in the diamictite matrix, a decrease in Mo/Pr ratios can be used to infer Mo loss. An ANOVA test reveals that there is a statistically significant difference between the δ^{98}Mo and the Mo/Pr ratio of the three populations at p=0.05. The Mo/Pr ratio is positively correlated with the δ^{98}Mo value of the diamictites such that the isotopically light diamictites also show the greatest Mo depletion (**Fig. 2**).

The TOC data are presented in Table 1 and Figure S3 in the supplementary material. All TOC values are very low (≤ 0.3 wt%) and there is no clear trend between TOC abundance and δ^{98}Mo for the diamictites.

4. Discussion

We present the first temporally constrained δ^{98}Mo values of the weathered UCC, which record the onset of oxidative weathering and potentially the growth of biomass on land. The glaciers that

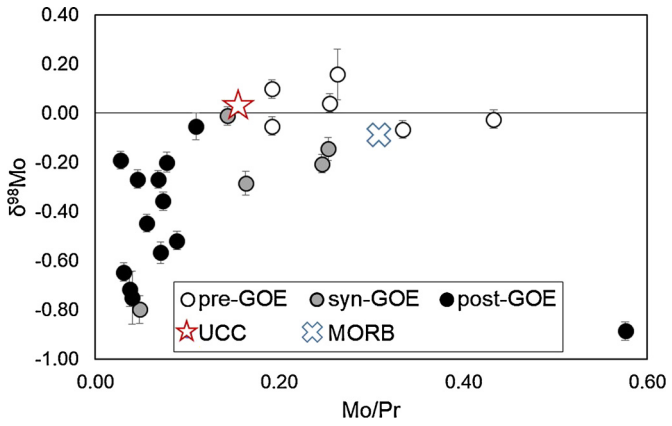

Fig. 2. Plot of Mo/Pr ratio versus δ^{98}Mo. Average MORB [Mo]: Jenner and O'Neill (2012); Average MORB δ^{98}Mo: Bezard et al. (2016); Liang et al. (2017). Average UCC [Mo]: Rudnick and Gao (2013), Average UCC δ^{98}Mo: average pre-GOE value.

created these tills sampled both unweathered igneous/metamorphic rock and weathered regolith. Therefore, the glacial diamictites contain two main geochemical signals. The first is a "primary" crustal evolution signature that records the transition of the continental crust from predominant mafic to felsic lithologies from the Late Archean and Proterozoic (Taylor and McLennan, 1985; Condie, 1993; Gaschnig et al., 2016). Overprinted on this primary signature is a secondary chemical weathering signature, which is reflected in Sr loss, elevated chemical index of alteration, and low δ^{7}Li (Gaschnig et al., 2016; Li et al., 2016). Therefore, the temporal δ^{98}Mo trend observed in the diamictites could result from two processes: 1) isotope fractionation generated during crustal differentiation as the UCC evolves from mafic to felsic, and/or 2) isotope fractionation induced during weathering/removal of Mo from the UCC.

4.1. Fractionation during crustal differentiation and compositional evolution

The "syn-" and "post-GOE" diamictites are isotopically lighter and have a lower Mo/Pr than the pre-GOE diamictites. While these observations could reflect a shift in the geochemistry of the "primary" igneous crust as it evolved from a more mafic to a more felsic composition, we explain below that this is likely not the case.

The δ^{98}Mo signature of the modern un-weathered UCC is surprisingly difficult to pin down. Upper crustal igneous rocks and molybdenite grains display a wide range of δ^{98}Mo values, encompassing almost the entire range of fractionation seen in river and marine environments (Breillat et al., 2014). Archean komatiites (average δ^{98}Mo = −0.21 ± 0.28‰ 2σ; Greber et al. (2015) and peridotites (–0.22 ± 0.06‰ 2σ; Liang et al., 2017) are isotopically lighter than mafic to felsic igneous rocks. Felsic igneous rocks vary from −0.35‰ to +0.59‰ (Freymuth et al., 2016; Voegelin et al., 2014; Yang et al., 2017; 2015), excluding samples affected by hydrothermal activity, while MORB (average −0.09 ± 0.02‰ 2σ) and OIB (average −0.14 ± 0.06‰ 2σ) tend to be relatively lighter than most felsic igneous rocks (Bezard et al., 2016; Liang et al., 2017). While no Mo isotope fractionation was observed by Yang et al. (2015) during igneous differentiation in an anhydrous intraplate setting, isotopic fractionation is proposed to occur in subduction zones due to crystallization of Mo-bearing minerals, which leaves arc magmas – therefore the UCC – isotopically heavier than mafic and ultramafic rocks (Voegelin et al., 2014; König et al., 2016; Wille et al., 2018). Estimates for the average modern igneous UCC range between +0.05‰ and +0.15‰ (Voegelin et al., 2014; Yang et al., 2017; Willbold and Elliott, 2017).

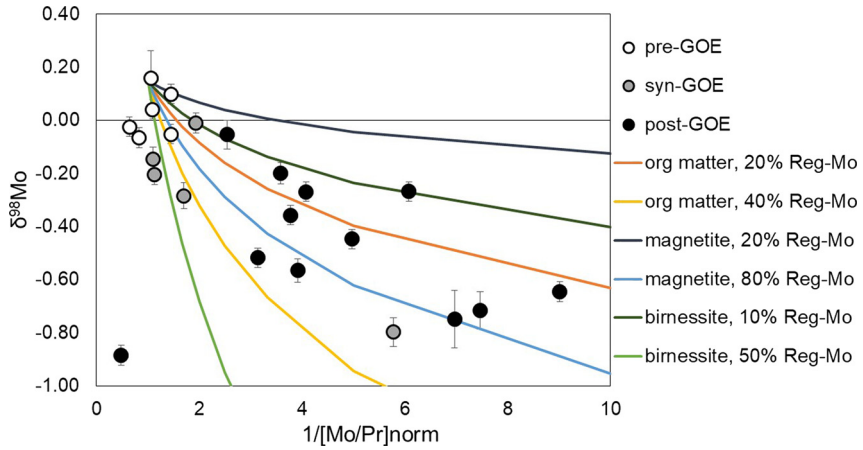

Fig. 3. Results of the Rayleigh fractionation and mixing models are shown with colored lines. Endmember fractionation factors from Goldberg et al. (2009) are used, representing Mo adsorption to magnetite ($\alpha = 1.0006$), organic matter ($\alpha = 1.0017$), and birnessite ($\alpha = 1.0024$). A range of proportions of Mo derived from the regolith are denoted as % Reg-Mo. Following Liu et al. (2013), the results of the model are plotted against $1/[Mo/Pr]_{norm}$, i.e. 1/F.

Because arc magmas can be significantly isotopically heavier than the mantle and MORB (König et al., 2016; Wille et al., 2018), we would expect the evolution from a more mafic to more felsic continental crust to shift the UCC to heavier values with time. However, the secular trend recorded in the diamictites shows the opposite. The pre-GOE diamictites fall within the range of average modern continental igneous rocks, while the younger samples are isotopically lighter. Therefore, we conclude that the trend to lighter isotope values over time as recorded in the diamictites is not a product of igneous differentiation and the compositional evolution of the "primary" UCC.

4.2. Fractionation due to oxidative weathering and Mo retention in soils

The decrease in the δ^{98}Mo values of the UCC with time is best explained by increased fractionation during oxidative weathering and subsequent Mo retention in soils. Today, molybdenum is removed from the exposed upper crust during oxidative weathering, and transported in solution to rivers and eventually oceans, resulting in authigenic Mo enrichments in marine sediments (Miller et al., 2011). Marine sediments enriched in Mo above UCC values (~1.1 ppm: Rudnick and Gao, 2013) appear in the rock record around the time of the GOE, suggesting there was limited oxidative weathering and Mo removal from the UCC before the GOE (Anbar et al., 2007; Scott et al., 2008; Wille et al., 2013). Complementary to the marine record, the diamictites record Mo loss from the UCC just after the GOE (Gaschnig et al., 2014), providing independent evidence for the hypothesis that Mo is transported from the UCC to oceans during oxidative weathering. As oxidative weathering increased after the GOE and Neoproterozoic Oxidation Event (NOE, ~550 Ma), more oxidized Mo was available for fractionation in the weathering environment, consistent with the secular δ^{98}Mo trend of the diamictites. Because Mo is not strongly depleted from the UCC relative to Pr before the GOE (Gaschnig et al., 2014), we can conclude that these samples represent "primary" igneous crust and the δ^{98}Mo value of Archean UCC is +0.03‰ (±0.18). This is within error of modern estimates of the UCC (see previous section).

Fractionation of Mo isotopes by adsorption on Fe-Mn oxides and organic matter has been proposed to explain the heavy riverine and seawater δ^{98}Mo signature (Archer and Vance, 2008; Siebert et al., 2003), and we show here that this *in-situ* fractionation is observed in the continental record beginning at the time of the GOE. Molybdenum isotope fractionation during weathering likely occurs by selective adsorption of isotopically light Mo onto Fe-Mn oxides or organic matter (OM) in the weathering profile. Fractionation between oxides and organic matter has been determined empirically and reported in multiple laboratory studies where isotopically light Mo is adsorbed by oxides or organic matter, while the Mo that remains in solution is relatively heavy (Barling et al., 2001; Barling and Anbar, 2004; Wasylenki et al., 2008; Goldberg et al., 2009; King et al., 2018). Experimental fractionation factors have been derived for the Mn-oxide birnessite (Wasylenki et al., 2008), the Fe-oxides hematite, magnetite, ferrihydrite, and goethite (Goldberg et al., 2009), and humic acid (King et al., 2018). We use these experimentally-derived fractionation factors to model the observed isotope fractionation in the diamictites.

4.2.1. Modeling the data

Rayleigh fractionation modelling was used to investigate whether incorporation of light Mo onto Fe-Mn oxides and/or organic matter in regolith can explain the isotopically light Mo observed in the diamictites. To build the model, we assume that all initial Mo is derived from igneous bedrock and that fractionation occurs in an oxidized weathering environment as aqueous Mo partitions between fluid that removes Mo from the system (e.g., groundwater) and oxides and/or organic matter that form in the weathered regolith. Dissociation and protonation of MoO_4^{2-} to MoO_3 or $MoO_3(H_2O)_3$ and subsequent adsorption to regolith-bound oxides or organic matter incorporates light Mo (Tossell, 2005; Wasylenki et al., 2008), resulting in the removal of isotopically heavy Mo in groundwater. Here the oxides/organic matter that sequester Mo are termed "regolith" as we assume that all Mo retained in the weathered regolith is adsorbed to these phases. Following the calculations of Liu et al. (2013) and Rudnick et al. (2004), isotope fractionation is modeled using equation (1) where α is the experimentally determined fractionation factor (fluid/mineral) and F represents the fraction of Mo retained in the regolith (**Fig. 3**).

$$\delta^{98}Mo_{regolith} = (\delta^{98}Mo_{bedrock} + 1000) * F^{(\alpha-1)} - 1000 \quad (1)$$

Fractionation factors derived from experimental work range from 1.0006 (magnetite – fluid fractionation; Goldberg et al., 2009) to 1.0024 (birnessite – fluid fractionation; Wasylenki et al., 2008) which encompasses the range of fractionation observed from adsorption onto organic matter (1.0017; King et al., 2018). Following Liu et al. (2013), we visualize the results of the Rayleigh model against the inverse of a normalized Mo/Pr ratio where $Mo/Pr_{norm} = Mo/Pr_{diamictite}/Mo/Pr_{bedrock}$, or in other words, 1/F (**Fig. 3**, **Fig. S1**). As we do not know the isotopic composition of the bedrock lithologies that were weathered and incorporated into the diamictites, we assume a starting igneous bedrock value of 0.03‰ and a

starting Mo/Pr ratio of 0.28, which are the pre-GOE averages of diamictites that have not lost and fractionated Mo. This calculation gives the δ^{98}Mo signature of the weathered regolith that contains Mo adsorbed to oxides and/or organic matter, assuming complete Mo mobilization from the UCC.

As the diamictites are likely a mixture of weathered regolith *and* un-weathered, un-fractionated bedrock, the results of the Rayleigh equation alone are a poor fit to the diamictite data (Supplementary Figure S1). The diamictites likely sampled variable amounts of unweathered bedrock which would dilute the expected Mo isotope signature induced by weathering. To account for variable amounts of un-weathered bedrock incorporated into the diamictites, we include unfractionated igneous bedrock (δ^{98}Mo = 0.03, Mo/Pr = 0.28) in a mixing model (equation (2)) where X indicates the proportion of regolith and bedrock, summing to one. We vary these proportions to generate curves that match the diamictite data (**Fig. 3**).

$$\delta^{98}Mo_{diamictite} = \left(\delta^{98}Mo_{regolith}\right) * X_{regolith} + (0.03‰) * X_{bedrock} \quad (2)$$

Here the results of the Rayleigh equation ($\delta^{98}Mo_{regolith}$) are used to calculate the expected diamictite isotope signature. The results of this mixing model support the observations in the diamictites (**Fig. 3**) which suggests that the syn- and post-GOE diamictites are mixtures of weathered regolith with fractionated Mo and un-weathered bedrock.

We can use the chemical index of alteration (CIA) to estimate the proportion of bedrock to regolith and confirm that variable proportions are present in these diamictites, as suggested by the results of the modeling equations. If we assume that granitic bedrock has a CIA of 52 and highly weathered regolith has a CIA of 90 (calculated from saprolites from Rudnick et al., 2004), we can build a mixing model (**Eq.** (3)), where X = proportion of bedrock, solved for in the equation. Using the chemical composition of multiple rocks to calculate the CIA of a mixture of those two lithologies results in a mixing line that is not purely linear (see supplementary Figure S2), however it is close enough that we can use the following equation to model mixing.

$$CIA = X\,(52) + (1 - X)(90) \quad (3)$$

The results of this calculation show that the syn- and post-GOE samples contain highly variable proportions of bedrock to regolith (between 5 and 79% weathered regolith) (**Table 2**, **Fig. 4**). These variable mixtures of bedrock to regolith partially explain the spread observed in the δ^{98}Mo and Mo, data as well as the apparent outliers like the Duitschland diamictite (**Fig. 1A**), which has a very high proportion of weathered regolith relative to the other syn-GOE samples (**Fig. 4**). This sample may, thus, provide a more accurate record of the δ^{98}Mo signature of soils and sediment at the time of the GOE, while the other syn-GOE diamictites have a δ^{98}Mo signature that has been diluted by isotopically heavier bedrock. The syn-GOE Duitschland diamictite can be compared to the pre-GOE Makganyene diamictite. Both contain similarly high proportions of weathered material, yet show very different δ^{98}Mo values. The Δ^{98}Mo between the two samples is 0.90‰, suggesting that the onset of oxidative weathering at ~2.4 Ga strongly fractionated Mo isotopes in the younger Duitschland sample. The degree of fractionation recorded by the syn-GOE Duitschland diamictite resembles that of more modern 300 Ma diamictites. These data may suggest that although oxygen levels are thought to have been low throughout the Proterozoic, a spike of atmospheric oxygen similar to levels recorded on a more modern Earth may have existed to strongly fractionate Mo isotopes at ~2.4 Ga (Lyons et al., 2014). Alternatively, this could reflect that at the start of the GOE, there was a larger proportion of oxidizable material at the Earth's surface that quickly weathered to release more Mo than later stages of the GOE.

Table 2
Results of "un-mixing" calculation using the CIA of each diamictite.

Sample	age Rel-GOE	CIA	proportion	
			% bedrock	% regolith
Mozaan	pre	74	42	58
Afrkiander	pre	77	34	66
Coronation	pre	78	32	68
Promise	pre	75	39	61
Ramsay Lake	pre	67	61	39
Makganyene	pre	89	3	97
Bruce	syn	61	76	24
Duitschland	syn	82	21	79
Gowganda	syn	57	87	13
Bottle Creek	syn	58	84	16
Timeball	syn	66	63	37
Kaigas	post	57	87	13
Konnarock	syn	56	89	11
Gaskiers	post	57	87	13
Pocatello	post	66	63	37
Nantuo	post	65	66	34
Gucheng	post	67	61	39
Blaubeker	post	59	82	18
Chuos	post	58	84	16
Numees	post	54	95	5
Ghaub	post	64	68	32
Bolivia	post	70	53	47
Dwyka East	post	56	89	11
Dwyka West	post	65	66	34

4.3. Other oxidative weathering signatures

Of the entire trace element suite measured in the diamictites by Gaschnig et al. (2016), negative correlations are observed for δ^{98}Mo vs. [Ba] and Mo vs. Th/U ($R^2 = 0.75$, excluding Duitschland and West Dywka as outliers and $R^2 = 0.63$, excluding West Dwyka, respectively) in the diamictites (**Fig. 5**). While these correlations may reflect changing UCC composition, we suggest instead that may also be influenced by oxidative weathering resulting from changing atmospheric conditions at the time of the GOE. The correlation between Th/U and δ^{98}Mo shows that post-GOE and syn-GOE samples are isotopically lighter and have a higher Th/U than pre-GOE samples. As U is oxidized to its hexavalent state, it becomes soluble, like Mo. Therefore, an increase in Th/U over time may suggest U is being removed from the continents as soluble U^{6+}. This is supported by U enrichments observed in black shales over time (Partin et al., 2013).

The negative correlation observed between δ^{98}Mo and Ba may also be explained by a change in atmosphere composition, in addition to a changing UCC composition. Widespread stabilization of barite ($BaSO_4^{2-}$) in sediments may have caused an increase in the Ba concentration of weathered regolith sampled by diamictites over time, due to the increase abundance of oxidized sulfur in the form of sulfate (Canfield, 2005). We conclude that the inverse correlations of Th/U and Ba concentrations with δ^{98}Mo are a result of both changing UCC composition and increased O_2 levels, which preferentially removed U^{6+} from UCC, and retained Ba in sulfate deposits following the GOE.

4.4. The role of Fe-Mn oxides and organic matter

Given our data and the results of the Rayleigh fractionation modeling, we conclude that Mo isotopes in the diamictites record the onset of oxidative weathering at the time of the GOE, as oxygen is needed to liberate Mo from the crust. We cannot confidently

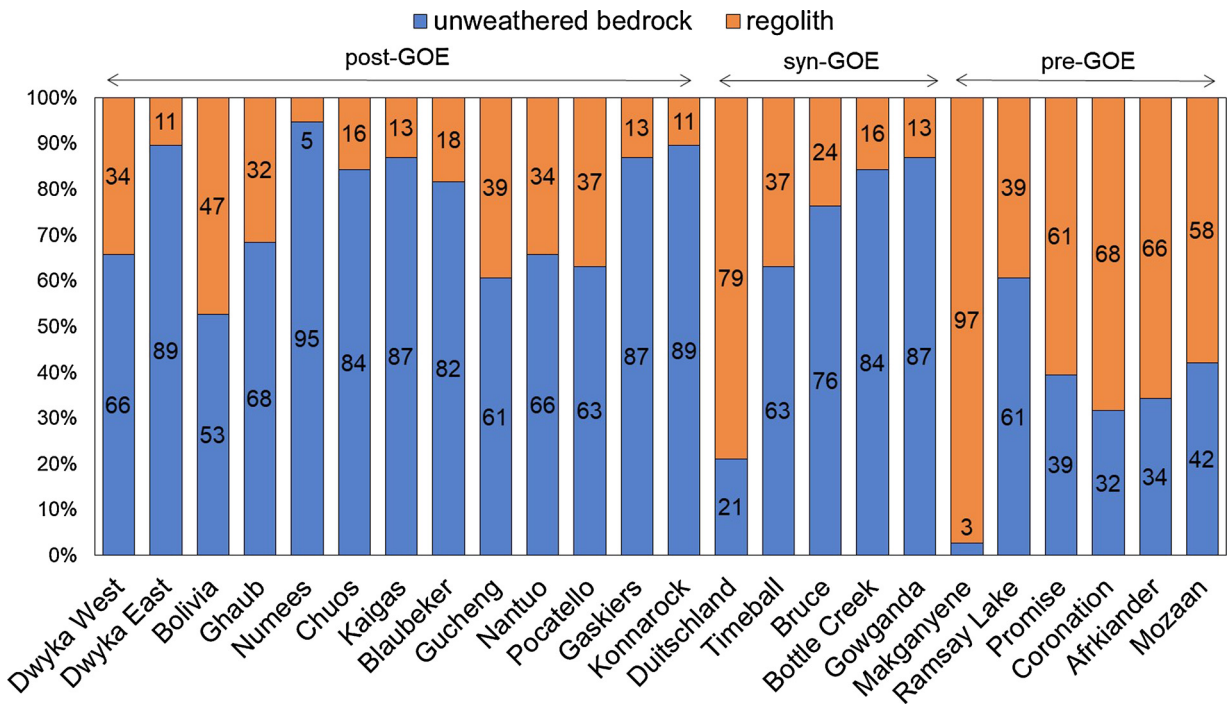

Fig. 4. Calculated proportions of weathered regolith and unweathered bedrock in the diamictites. Results were obtained using a mixing model between a "weathered" endmember with a theoretical CIA of 90 and an "unweathered" endmember with a theoretical CIA of 52.

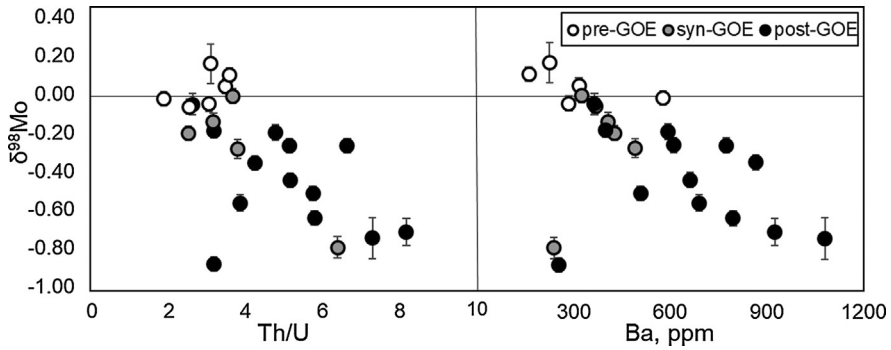

Fig. 5. Correlations between δ^{98}Mo, Th/U and Ba.

determine whether Fe-Mn oxides or organic matter are the dominant phase that incorporates light Mo isotopes in the regolith, because low grade metamorphism has overprinted the original mineralogy of the samples. However, it is very likely that oxidative continental weathering results in Mo isotope fractionation due to adsorption on to one or both of these phases. There is a slightly more robust relationship between δ^{98}Mo and Fe_2O_3 and MnO than between δ^{98}Mo and organic matter (supplementary figures S3 and S4), suggesting that Fe-Mn oxides may play a stronger role in long-term retention of light Mo in weathered regolith. The presence of Fe-Mn oxides in soils is, in itself, an oxidative weathering signature, as these phases are not expected to be stable under an anoxic atmosphere (Murakami et al., 2011). Therefore, the correlation between the stabilization of oxides in soils after the GOE and the onset of Mo isotope fractionation during weathering is expected.

If Mo adsorption onto organic matter is an important isotope-fractionating mechanism, then the diamictites may also record an increase in continental biomass in addition to oxidative mobilization of Mo. The shift to lower δ^{98}Mo in the syn-GOE diamictites could therefore represent a slight increase in continental biomass following the GOE. This may have contributed to low atmospheric oxygen levels in the Proterozoic (Kump, 2013).

4.5. Implications for δ^{98}Mo of river water through time

We show here that post-GOE weathered continental crust is isotopically light, with respect to Mo, and provides a complementary reservoir for modern rivers that are isotopically heavy relative to the UCC (Archer and Vance, 2008). Some researchers attribute this to adsorption of light Mo isotopes onto oxides in regolith during continental weathering (Archer and Vance, 2008; Pearce et al., 2010), while others propose that heavy riverine values instead reflect weathering of a source that's heavier than average continental crust, such as molybdenite (Dahl et al., 2011; Neubert et al., 2011). The temporal trend of the UCC, as recorded by diamictites, is a mirror image of that of marine shales (**Fig. 6**) suggesting that mass balance is maintained over time. Thus, we hypothesize that the Mo isotope signature of Archean rivers was likely indistinguishable from Archean crust. Archean rivers likely would have been nearly devoid of Mo without oxidative weathering to liberate it from molybdenite in the crust. However, some Mo may have been released from weathering of basaltic or rhyolitic glass (Greaney et al., 2018) or other Mo bearing phases that weather congruently under an anoxic atmosphere. Liberation of small amounts of Mo and the lack of Fe,Mn-oxides or organic matter in pre-GOE soils (Murakami et al., 2011) would have resulted in an Archean river-

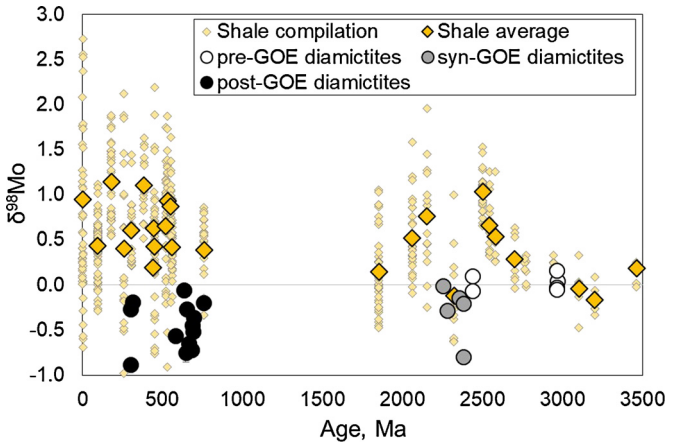

Fig. 6. Marine shales and sediments in yellow diamonds show the complementary signature to the weathered upper crust as represented by the diamictites. The average δ^{98}Mo value for each shale group is presented in the larger diamond. References for the shale data can be found in the supplementary material. (For interpretation of the colors in the figure(s), the reader is referred to the web version of this article.)

ine Mo isotopic signature identical to that of the Archean crust (~0.03‰). This inference is further supported by pre-GOE marine shales that show a similar Mo isotopic signature, within error (average δ^{98}Mo = +0.18 ± 0.22 ‰), to the pre-GOE diamictites and estimates of the igneous crust (**Fig. 6**). If this hypothesis is true, it would have implications for evaluating Mo isotope fractionation observed in marine basins at this time, however further studies are needed to test this idea.

5. Conclusions

A secular change in δ^{98}Mo of the weathered UCC is observed in glacial diamictites that were deposited between 2900 and 300 Ma. The δ^{98}Mo signature of the diamictites that formed before the GOE (average +0.03‰) is similar to the range that encompasses continental igneous rocks while the diamictites that formed during and after the GOE (average −0.29‰ and −0.45‰, respectively) are significantly lighter. We use the pre-GOE data to establish that the δ^{98}Mo signature of the "primary" Archean continental crust, before undergoing Mo removal and fractionation via oxidative weathering, is +0.03‰. The shift in Mo isotopes to lighter values after the GOE is due to fractionation during oxidative weathering, as isotopically light Mo is adsorbed onto authigenic/residual Fe-Mn oxides or organic matter in soils and sediment. Therefore, we conclude that Mo isotopes in diamictites reliably record Earth's surface oxygenation, including near-modern pO_2 at 2.4 Ga, as evidenced by the Duistchland diamictite. Finally, mass balance modeling suggests that the UCC is the complementary reservoir to Mo in rivers and oceans, independently verifying the isotopically heavy nature of Mo sources to the ocean through time.

Declaration of competing interest

The authors declare that they have no known competing financial interests or personal relationships that could have appeared to influence the work reported in this paper.

Acknowledgements

We thank Jay Kaufman for assistance with TOC data collection and Gwenyth Gordon for assistance during Mo isotope measurements. This work was supported by National Science Foundation Grants EAR 1321954 (Rudnick, PI), EAR 133810 (Anbar, PI; Rudnick, Co-PI) and EAR 1757313 (Rudnick, PI).

Appendix A. Supplementary material

Supplementary material related to this article can be found online at https://doi.org/10.1016/j.epsl.2020.116083.

References

Anbar, A.D., Duan, Y., Lyons, T.W., Arnold, G.L., Kendall, B., Creaser, R.A., Kaufman, A.J., Gordon, G.W., Scott, C., Garvin, J., Buick, R., 2007. A whiff of oxygen before the great oxidation event? Science 80 (317), 1903–1906. https://doi.org/10.1126/science.1140325.

Archer, C., Vance, D., 2008. The isotopic signature of the global riverine molybdenum flux and anoxia in the ancient oceans. Nat. Geosci. 1, 597–600. https://doi.org/10.1038/ngeo282.

Barling, J., Anbar, A.D., 2004. Molybdenum isotope fractionation during adsorption by manganese oxides. Earth Planet. Sci. Lett. 217, 315–329. https://doi.org/10.1016/S0012-821X(03)00608-3.

Barling, J., Arnold, G.L., Anbar, A.D., 2001. Natural mass-dependent variations in the isotopic composition of molybdenum. Earth Planet. Sci. Lett. 193, 447–457. https://doi.org/10.1016/S0012-821X(01)00514-3.

Bezard, R., Fischer-Gödde, M., Hamelin, C., Brennecka, G.A., Kleine, T., 2016. The effects of magmatic processes and crustal recycling on the molybdenum stable isotopic composition of Mid-Ocean Ridge Basalts. Earth Planet. Sci. Lett. 453, 171–181. https://doi.org/10.1016/j.epsl.2016.07.056.

Breillat, N., Guerrot, C., Marcoux, E., Négrel, P., 2014. A new global database of δ^{98}Mo in molybdenites: a literature review and new data. J. Geochem. Explor. 161, 1–15. https://doi.org/10.1016/j.gexplo.2015.07.019.

Canfield, D.E., 2005. The early history of atmospheric oxygen: homage to Robert M. Garrels. Annu. Rev. Earth Planet. Sci. 33, 1–36. https://doi.org/10.1146/annurev.earth.33.092203.122711.

Condie, K.C., 1993. Chemical composition and evolution of the upper continental crust: contrasting results from surface and shales 104, 1–37. https://doi.org/10.1016/0009-2541(93)90140-E.

Dahl, T.W., Canfield, D.E., Rosing, M.T., Frei, R.E., Gordon, G.W., Knoll, A.H., Anbar, A.D., 2011. Molybdenum evidence for expansive sulfidic water masses in ~750 Ma oceans. Earth Planet. Sci. Lett. 311, 264–274. https://doi.org/10.1016/j.epsl.2011.09.016.

Duan, Y., Anbar, A.D., Arnold, G.L., Lyons, T.W., Gordon, G.W., Kendall, B., 2010. Molybdenum isotope evidence for mild environmental oxygenation before the great oxidation event. Geochim. Cosmochim. Acta 74, 6655–6668. https://doi.org/10.1016/j.gca.2010.08.035.

Freymuth, H., Elliott, T., van Soest, M., Skora, S., 2016. Tracing subducted black shales in the Lesser Antilles arc using molybdenum isotope ratios. Geology 44, 987–990. https://doi.org/10.1130/G38344.1.

Gaschnig, R.M., Rudnick, R.L., McDonough, W.F., Kaufman, A.J., Hu, Z., Gao, S., 2014. Onset of oxidative weathering of continents recorded in the geochemistry of ancient glacial diamictites. Earth Planet. Sci. Lett. 408, 87–99. https://doi.org/10.1016/j.epsl.2014.10.002.

Gaschnig, R.M., Rudnick, R.L., McDonough, W.F., Kaufman, A.J., Valley, J.W., Hu, Z., Gao, S., Beck, M.L., 2016. Compositional evolution of the upper continental crust through time, as constrained by ancient glacial diamictites. Geochim. Cosmochim. Acta 186, 316–343. https://doi.org/10.1016/j.gca.2016.03.020.

Goldberg, T., Archer, C., Vance, D., Poulton, S.W., 2009. Mo isotope fractionation during adsorption to Fe (oxyhydr)oxides. Geochim. Cosmochim. Acta 73, 6502–6516. https://doi.org/10.1016/j.gca.2009.08.004.

Goldberg, T., Gordon, G., Izon, G., Archer, C., Pearce, C.R., McManus, J., Anbar, A.D., Rehkämper, M., 2013. Resolution of inter-laboratory discrepancies in Mo isotope data: an intercalibration. J. Anal. At. Spectrom. 28, 724. https://doi.org/10.1039/c3ja30375f.

Greaney, A.T., Rudnick, R.L., Gaschnig, R.M., Whalen, J.B., Luais, B., Clemens, J.D., 2018. Geochemistry of molybdenum in the continental crust. Geochim. Cosmochim. Acta 238, 36–54. https://doi.org/10.1016/j.gca.2018.06.039.

Greber, N.D., Puchtel, I.S., Nägler, T.F., Mezger, K., 2015. Komatiites constrain molybdenum isotope composition of the Earth's mantle. Earth Planet. Sci. Lett. 421, 129–138. https://doi.org/10.1016/j.epsl.2015.03.051.

Gumsley, A.P., Chamberlain, K.R., Bleeker, W., Söderlund, U., de Kock, M.O., Larsson, E.R., Bekker, A., 2017. Timing and tempo of the great oxidation event. Proc. Natl. Acad. Sci. 114, 1811–1816. https://doi.org/10.1073/pnas.1608824114.

Jenner, F.E., O'Neill, H.S.C., 2012. Analysis of 60 elements in 616 ocean floor basaltic glasses. Geochem. Geophys. Geosyst. 13, 1–11. https://doi.org/10.1029/2011GC004009.

Johnson, A.C., Romaniello, S.J., Reinhard, C.T., Gregory, D.D., Garcia-robledo, E., Peter, N., Canfield, D.E., Lyons, T.W., Anbar, A.D., 2019. Experimental determination of pyrite and molybdenite oxidation kinetics at nanomolar oxygen concentrations. Geochim. Cosmochim. Acta 249, 160–172. https://doi.org/10.1016/j.gca.2019.01.022.

Kendall, B., Dahl, T.W., Anbar, A.D., 2017. The stable isotope geochemistry of molybdenum. Rev. Mineral. Geochem. 82, 683–732. https://doi.org/10.2138/rmg.2017.82.16.

King, E.K., Perakis, S.S., Pett-Ridge, J.C., 2018. Molybdenum isotope fractionation during adsorption to organic matter. Geochim. Cosmochim. Acta 222, 584–598. https://doi.org/10.1016/j.gca.2017.11.014.

King, E.K., Thompson, A., Chadwick, O.A., Pett-Ridge, J.C., 2016. Molybdenum sources and isotopic composition during early stages of pedogenesis along a basaltic climate transect. Chem. Geol. 445, 54–67. https://doi.org/10.1016/j.chemgeo.2016.01.024.

König, S., Wille, M., Voegelin, A., Schoenberg, R., 2016. Molybdenum isotope systematics in subduction zones. Earth Planet. Sci. Lett. 447, 95–102. https://doi.org/10.1016/j.epsl.2016.04.033.

Li, S., Gaschnig, R.M., Rudnick, R.L., 2016. Insights into chemical weathering of the upper continental crust from the geochemistry of ancient glacial diamictites. Geochim. Cosmochim. Acta 176, 96–117. https://doi.org/10.1016/j.gca.2015.12.012.

Li, S., Junkin, W.L., Gaschnig, R.M., Ash, R.D., Piccoli, P.M., Candela, P.A., Rudnick, R.L., 2019. Molybdenum contents of sulfides in ancient glacial diamictites: implications for molybdenum delivery to the oceans prior to the great oxidation event. Geochim. Cosmochim. Acta 176, 96–117. https://doi.org/10.1016/j.gca.2019.09.011.

Liang, Y.H., Halliday, A.N., Siebert, C., Fitton, J.G., Burton, K.W., Wang, K.L., Harvey, J., 2017. Molybdenum isotope fractionation in the mantle. Geochim. Cosmochim. Acta 199, 91–111. https://doi.org/10.1016/j.gca.2016.11.023.

Liu, X., Rudnick, R.L., Mcdonough, W.F., Cummings, M.L., 2013. Influence of chemical weathering on the composition of the continental crust: insights from Li and Nd isotopes in bauxite profiles developed on Columbia River Basalts. Geochim. Cosmochim. Acta 115, 73–91. https://doi.org/10.1016/j.gca.2013.03.043.

Lyons, T.W., Reinhard, C.T., Planavsky, N.J., 2014. The rise of oxygen in Earth's early ocean and atmosphere. Nature 506, 307–315. https://doi.org/10.1038/nature13068.

Marks, J.A., Perakis, S.S., King, E.K., Pett-Ridge, J., 2015. Soil organic matter regulates molybdenum storage and mobility in forests. Biogeochemistry 125, 167–183. https://doi.org/10.1007/s10533-015-0121-4.

Miller, C.A., Peucker-Ehrenbrink, B., Walker, B.D., Marcantonio, F., 2011. Re-assessing the surface cycling of molybdenum and rhenium. Geochim. Cosmochim. Acta 75, 7146–7179. https://doi.org/10.1016/j.gca.2011.09.005.

Murakami, T., Sreenivas, B., Sharma, Das S., Sugimori, H., 2011. Quantification of atmospheric oxygen levels during the paleoproterozoic using paleosol compositions and iron oxidation kinetics. Geochim. Cosmochim. Acta 75, 3982–4004. https://doi.org/10.1016/j.gca.2011.04.023.

Neubert, N., Heri, A.R., Voegelin, A.R., Nägler, T.F., Schlunegger, F., Villa, I.M., 2011. The molybdenum isotopic composition in river water: constraints from small catchments. Earth Planet. Sci. Lett. 304, 180–190.

Partin, C.A., Bekker, A., Planavsky, N.J., Scott, C.T., Gill, B.C., Li, C., Podkovyrov, V., Maslov, A., Konhauser, K.O., Lalonde, S.V., Love, G.D., Poulton, S.W., Lyons, T.W., 2013. Large-scale fluctuations in Precambrian atmospheric and oceanic oxygen levels from the record of U in shales. Earth Planet. Sci. Lett. 369–370, 284–293. https://doi.org/10.1016/j.epsl.2013.03.031.

Pearce, C.R., Burton, K.W., von Strandmann, P.A.E.P., James, R.H., Gíslason, S.R., 2010. Molybdenum isotope behaviour accompanying weathering and riverine transport in a basaltic terrain. Earth Planet. Sci. Lett. 295, 104–114. https://doi.org/10.1016/j.epsl.2010.03.032.

Romaniello, S.J., Herrmann, A.D., Anbar, A.D., 2016. Syndepositional diagenetic control of molybdenum isotope variations in carbonate sediments from the Bahamas. Chem. Geol. 438, 84–90. https://doi.org/10.1016/j.chemgeo.2016.05.019.

Rudnick, R.L., Gao, S., 2013. Composition of the Continental Crust, 2nd ed. Treatise on Geochemistry. Elsevier Ltd. https://doi.org/10.1016/B978-0-08-095975-7.00301-6.

Rudnick, R.L., Tomascak, P.B., Njo, H.B., Gardner, L.R., 2004. Extreme lithium isotopic fractionation during continental weathering revealed in saprolites from South Carolina. Chem. Geol. 212, 45–57. https://doi.org/10.1016/j.chemgeo.2004.08.008.

Scott, C., Lyons, T.W., Bekker, A., Shen, Y., Poulton, S.W., Chu, X., Anbar, A.D., 2008. Tracing the stepwise oxygenation of the Proterozoic ocean. Nature 452, 456–459. https://doi.org/10.1038/nature06811.

Siebert, C., Nägler, T.F., von Blanckenburg, F., Kramers, J.D., 2003. Molybdenum isotope records as a potential new proxy for paleoceanography. Earth Planet. Sci. Lett. 211, 159–171. https://doi.org/10.1016/S0012-821X(03)00189-4.

Siebert, C., Pett-Ridge, J.C., Opfergelt, S., Guicharnaud, R.A., Halliday, A.N., Burton, K.W., 2015. Molybdenum isotope fractionation in soils: influence of redox conditions, organic matter, and atmospheric inputs. Geochim. Cosmochim. Acta 162, 1–24. https://doi.org/10.1016/j.gca.2015.04.007.

Taylor, S.R., McLennan, S.M., 1985. The Continental Crust: Its Composition and Evolution. Blackwell, Oxford, pp. 1–312.

Tossell, J.A., 2005. Calculating the partitioning of the isotopes of Mo between oxidic and sulfidic species in aqueous solution. Geochim. Cosmochim. Acta 69, 2981–2993. https://doi.org/10.1016/j.gca.2005.01.016.

Voegelin, A.R., Pettke, T., Greber, N.D., von Niederhäusern, B., Nägler, T.F., 2014. Magma differentiation fractionates Mo isotope ratios: evidence from the Kos Plateau Tuff (Aegean Arc). Lithos 190–191, 440–448. https://doi.org/10.1016/j.lithos.2013.12.016.

Wang, Z., Ma, Z., Wei, G., Zeng, T., Li, L., Zhang, L., Deng, W., Xie, L., Liu, Z., 2018. Fe (hydro) oxide controls Mo isotope fractionation during the weathering of granite. Geochim. Cosmochim. Acta 226, 1–17.

Wasylenki, L.E., Rolfe, B.A., Weeks, C.L., Spiro, T.G., Anbar, A.D., 2008. Experimental investigation of the effects of temperature and ionic strength on Mo isotope fractionation during adsorption to manganese oxides. Geochim. Cosmochim. Acta 72, 5997–6005. https://doi.org/10.1016/j.gca.2008.08.027.

Willbold, M., Elliott, T., 2017. Molybdenum isotope variations in magmatic rocks. Chem. Geol. 449, 253–268. https://doi.org/10.1016/j.chemgeo.2016.12.011.

Wille, M., Nebel, O., Pettke, T., Vroon, P.Z., König, S., Schoenberg, R., 2018. Molybdenum isotope variations in calc-alkaline lavas from the Banda arc, Indonesia: assessing the effect of crystal fractionation in creating isotopically heavy continental crust. Chem. Geol. 485, 1–13. https://doi.org/10.1016/J.CHEMGEO.2018.02.037.

Wille, M., Nebel, O., Van Kranendonk, M.J., Schoenberg, R., Kleinhanns, I.C., Ellwood, M.J., 2013. Mo-Cr isotope evidence for a reducing Archean atmosphere in 3.46-2.76 Ga black shales from the Pilbara, Western Australia. Chem. Geol. 340, 68–76. https://doi.org/10.1016/j.chemgeo.2012.12.018.

Yang, J., Barling, J., Siebert, C., Fietzke, J., Stephens, E., Halliday, A.N., 2017. The molybdenum isotopic compositions of I-, S- and A-type granitic suites. Geochim. Cosmochim. Acta 205, 168–186. https://doi.org/10.1016/j.gca.2017.01.027.

Yang, J., Siebert, C., Barling, J., Savage, P., Liang, Y.H., Halliday, A.N., 2015. Absence of molybdenum isotope fractionation during magmatic differentiation at Hekla volcano, Iceland. Geochim. Cosmochim. Acta 162, 126–136. https://doi.org/10.1016/j.gca.2015.04.011.